NASA

Technical Memorandum 85118

SOFT X-RAY SPECTRAL OBSERVATIONS OF QUASARS AND HIGH X-RAY LUMINOSITY SEYFERT GALAXIES

R. Petre
R. F. Mushotzky
J. H. Krolik
S. S. Holt

(NASA-TM-85118) SOFT X-RAY SPECTRAL OBSERVATIONS OF QUASARS AND HIGH X-RAY LUMINOSITY SEYFERT GALAXIES (NASA) 53 p HC A04/MF A01
CSCL 03A

N84-14082

Unclas
G3/89 42611

November 1983

National Aeronautics and
Space Administration

Goddard Space Flight Center
Greenbelt, Maryland 20771

SOFT X-RAY SPECTRAL OBSERVATIONS OF QUASARS AND HIGH X-RAY LUMINOSITY SEYFERT GALAXIES

R. Petre[1], R.F. Mushotzky, J.H. Krolik[2], and S.S. Holt

Laboratory for High Energy Astrophysics
NASA/Goddard Space Flight Center
Greenbelt, Maryland 20771

ABSTRACT

We present results of the analysis of 28 Einstein SSS observations of 15 high X-ray luminosity ($L_X > 10^{43.5}$ erg s^{-1}) quasars and Seyfert type I nuclei. The 0.75-4.5 keV spectra are in general well fit by a simple model consisting of a power law plus absorption by cold gas. The average spectral index $\langle\alpha\rangle$ is 0.66±.36, consistent with $\langle\alpha\rangle$ for the spectrum of these objects above 2 keV. In all but one case, we find no evidence for intrinsic absorption, with an upper limit of 2×10^{21} cm^{-2}. We also find no evidence for partial covering of the active nucleus by dense, cold matter ($N_H > 10^{22}$ cm^{-2}); the average upper limit on the partial covering fraction is 0.5. There is no obvious correlation between spectral index and 0.75-4.5 keV X-ray luminosity (which ranges from 3×10^{43} to 10^{47} erg s^{-1}) or with other source

properties. The lack of intrinsic X-ray absorption allows us to place constraints on the density and temperature of the broad-line emission region, the narrow line emission region, and the intergalactic medium.

Subject headings: galaxies: nuclei--galaxies: Seyfert--Quasars--X-rays: sources--X-rays: spectra

Suggested running title: X-Ray Spectra of AGN

[1]NAS/NRC Research Associate

[2]Harvard/Smithsonian Center for Astrophysics, Cambridge, MA 02138

I. INTRODUCTION

Prior to the launch of the HEAO series of satellites, the study of X-ray emission from active galactic nuclei (AGN) was limited to little more than the identification and measurement of the luminosity of the brightest X-ray AGN. Approximately 20 X-ray emitting AGN were discovered by sounding rocket instruments and early X-ray satellite experiments (Uhuru, Ariel 5, SAS-C); of these, two were quasars (3C273 - Bowyer et al. 1970; and QSO 0241+622 - Apparao et al. 1978) and the majority of the remainder were Seyfert type I galaxies (Tananbaum et al. 1978; Elvis et al. 1978). Since the flux from even the brightest AGN is no more than 10^{-3} of the Crab, proportional counters with limited spectral resolution and pass bands (typically 2-10 keV) were unable to characterize their spectra.

The more sophisticated, wider bandpass proportional counters comprising the HEAO-1 A2 experiment doubled the catalog of detected AGN and facilitated the first systematic investigations of their X-ray spectral properties. Mushotzky et al. (1980,1983) reported that the spectra of the 14 most luminous Seyfert I galaxies ($L_X > 5 \times 10^{43}$ erg s^{-1}) are generally consistent with a single power law of index $\alpha \sim 0.7$ over more than a decade in energy (2-40 keV), with no apparent absorption from cold gas in the line of sight in excess of that expected from our own galaxy. Moreover, Mushotzky (1982) found that Narrow Emission Line Galaxies (NELG) appear to possess X-ray spectral slopes indistinguishable from those of Seyferts type I ($\alpha \sim 0.7 \pm 0.1$ for 14 SyI and 5 NELG), but are inherently less luminous and display evidence of cold gas with column densities of greater than 1×10^{22} cm^{-2} in the line of sight. Interestingly, the spectral indices of the two quasars sufficiently bright to permit spectroscopy by HEAO-1 A2 are inconsistent with this "universal" value: 3C 273 has a flatter slope ($\alpha = 0.4 \pm 0.02$; Worrall et al, 1979) and the

slope of 0O241+622 is marginally steeper (α = 0.9 (+0.5,-.03), Worrall et al. 1980). The X-ray spectral properties of BL Lac objects are clearly very different from those of the Seyfert type I nuclei (e.g. Holt 1981).

HEAO-2, the Einstein Observatory, carried in its focal plane array the Solid State Spectrometer (SSS), which was capable of carrying out high-sensitivity, moderate resolution spectroscopy in the 0.5-4.5 keV band. It was thus useful for investigating possible differences in the low energy AGN continuum spectra from their higher energy form (e.g., changes of spectral slope, evidence for absorption, line emission and edges). In this paper we discuss the soft X-ray spectral properties of the high X-ray luminosity AGN in the SSS data base: Seyferts type I and quasars. These are the objects in which no evidence of absorption was found in observations above 2 keV.

Our sample of high luminosity AGN consists of 15 sources: 3 quasars and 12 Seyferts. We find that with the moderate spectral resolution ($E/\Delta E \sim 20$) afforded by the SSS, the spectra of most of these display no strong features; they are best fit by a single power law plus absorption. The average spectral index of the sample is 0.66 ± 0.36. We find no strong evidence for a second spectral component, either thermal or non-thermal, with a single possible exception (3C 120). In addition, there is no evidence for absorbing material intrinsic to these sources with $N_H > 2 \times 10^{21}$ cm^{-2}.

Section II of this paper contains a description of the observations and the data reduction technique, while the results of model fitting to the spectra are presented in Section III. In Section IV, we compare our inferred spectral indices, column densities and fluxes to values obtained in other X-ray observations, and discuss the upper limits to X-ray-determined covering fractions (Holt et al. 1980). The implications of our measurements as regards the nature of the source of X-ray emission and the absorbing medium intrinsic

to the AGN are discussed in Section V. In Section VI we summarize our principal results and state our conclusions.

II. OBSERVATIONS AND ANALYSIS PROCEDURE

The SSS is a non-dispersive Si(Li) spectrometer with energy resolution of ~ 160 eV (FWHM) approximately independent of energy over its operating range of 0.5-4.5 keV. Detailed descriptions of the instrument can be found in Joyce et al. (1978) and Holt et al. (1979). Refinements in the understanding of systematic effects in the pulse-height spectra (detector background and ice buildup on the detector surface) now allow us to utilize nearly the full energy range of the instrument, with properly inflated errors in spectral parameters to account for the remaining uncertainties in the contribution of these contaminants. However, since weak sources, such as some of those discussed here, can suffer most from systematic errors that predominantly affect the four lowest pulse height channels (0.5-0.75 keV), these channels are excluded from all spectral analyses discussed here in order to generate a uniform response across the sample.

All SSS observations are accompanied by measurements using the coaligned Monitor Proportional Counter (MPC), providing coverage in the 1.5-10 keV band. Independent spectral fitting of the MPC data (Halpern 1982) provides a simultaneous extension of the observed spectral range to higher energies, with considerable overlap.

The AGN discussed here have been selected from the SSS observation catalog on the basis of their 2-10 keV luminosity: these are all the AGN with

L_{2-10} greater than 3×10^{43} erg s^{-1} that yielded useful data[3]. Fifteen AGN,

[3]Observations of three other high luminosity AGN, NRAO 530, 3C 279, and Ton 256, yielded no useful data. NRAO 530 and 3C 279 produced too low a signal, and HEAO-2 was mispointed 40' away from Ton 256.

all either quasars or Seyferts type I, satisfy this criterion. These objects are listed in Table 1, along with their positions, classifications, redshifts, and the specifics of each SSS observation. A total of 28 useful observations were carried out, averaging 6.8×10^3 s in duration. Accompanying the description of each observation is a quality flag. The observations fell naturally into three quality classes (1, 2 and 3, where 1 represents the high quality), depending on both the overall signal-to-noise of the data and the confidence with which systematic effects due to contamination by ice and instrumental background could be modelled. Each of the 28 observations satisfies the condition that the total number of counts in the pulse height spectrum ascribed to the source considerably exceeds those ascribed to background effects, in order that systematic uncertainties remain less significant than statistical uncertainties. In contrast, the signal-to-noise level in the MPC is ~ 1:15 for these sources.

While the energy resolution advantage of the SSS over the HEAO-1 A2 proportional counters (a factor of ~ 5 at 3 keV) is important for the identification of sharp features, the two instruments have roughly the same ratio of total energy range to FWHM resolution (~ 25). For the characterization of smooth continua, they are therefore equivalent for comparable errors in each FWHM energy bin. (The MPC, on the other hand, is distinctly inferior in this respect by a factor of 3).

Spectral model fitting of the SSS pulse height data is carried out via a technique described in detail elsewhere (see e.g. Holt et al. 1980). The starting point for all the data analysis described here is the assumption of a power-law continuum viewed through a uniform, cold absorbing gas of universal abundance. We have used the absorption model of Morrison and McCammon (1983), which includes the most up-to-date atomic cross sections and cosmic abundances. Uncertainties in systematic effects are treated like spectral fitting parameters, so that they act to increase the acceptable fit ranges of the interesting source parameters. If, and only if, the fit to a simple power-law spectrum is unacceptable, do we attempt a fit with more complicated models. Previously reported examples of such model refinements for AGN have been the postulation of a two-component power-law form for ESO 141-G55 (Mushotzky et al. 1980), and the suggestion that there is both nonuniformity and enhanced metallicity in cold gas absorption in the direction of NGC 4151 (Holt et al. 1980). Clearly, such refinements in general are merited only by data of high statistical quality that have been found inconsistent with a simple power-law fit.

III. RESULTS OF MODEL FITTING

a. Simple model (power law plus absorption)

Table 2 contains the best fit parameters for a single power law plus absorption model for each of the 28 observations. Columns in Table 2 represent the normalization, the spectral energy index α, the column density N_H, the ranges in α and N_H and the reduced chi-squared χ^2_ν. In all observations the number of degrees of freedom ν is equal to 58. Free parameters in the model are the normalization, α, N_H and a multiplier to a small, non-predictable component of the nominal background model. The ranges of α and N_H were defined using $(\chi^2_{min} + 6)$ which gives $\sim$ 90 percent confidence

limits for 3 interesting parameters or ~ 95 percent confidence limits for 2 interesting parameters (Lampton, Margon and Bowyer 1976); we chose such error bounds so that potential contamination by systematic effects is less likely to affect our conclusions than might less conservative limits. For most of the fits, however, the choice of a slightly less conservative set of confidence limits (i.e., χ^2_{min} + 4.6: 90 percent confidence for 2 interesting parameters) does not reduce the allowed range of α and N_H significantly.

As an illustration of the quality of the model fits to the data, the variation in data quality from source to source, and the level at which systematic and random errors come into play, we display in Figure 1 examples of data representing the three quality levels and their corresponding best fit spectra. For each data set displayed, the left panel shows the best fit pulse-height spectrum (solid line) overlayed on the actual pulse-height data, and the right panel shows the input photon spectrum deconvolved from instrumental response. Quality 1 data are represented by the second MCG 2-58-22 observation (1a-b) and IC 4329A (1 c-d). Note in both 1a and 1c the high quality of the data (small error bars across the 0.75 - 4.5 keV band) and the fidelity with which the best fit spectrum reproduces the data. Quality 2 data are represented by III Zwicky 2(1e-f). Observations of this quality have lower signals or less exposure than the best quality observations and thus tend to have large error bars at higher energies; consequently, the allowed range of fitting parameters to quality 2 data tend to be larger than for quality 1 data. 3C 111 (1 g-h) and NRAO 140 (1 i-j) exemplify the lowest quality data, where the weak source fluxes and systematic uncertainties tend to produce relatively wide acceptable parameter ranges and/or large values of χ^2_ν. Since these quality 3 data are of insufficient quality to merit fitting with more detailed spectra, we will restrict our modelling of them to

the simple case (power law plus absorption).

In Figure 2 we have plotted the integral χ^2_ν distribution of our single power law fits. The dashed curve represents an integral χ^2_ν distribution for 28 observations and $\nu = 58$. In order to determine whether our fits are consistent with the χ^2_ν distribution, we have applied the Kolmogorov-Smirnov test to the histogram in Figure 2. The resulting probability of 0.63 suggests that our fits are in fact consistent with a χ^2_ν distribution Therefore, when the spectra of the AGN in our sample are considered collectively, the simplest model consistent with previous broader band observations (Rothschild et al. 1983), a power law plus absorption, provides an adequate description of them.

b. Multicomponent models

Although we cannot reject the hypothesis that the simple model discussed above provides an adequate fit to our spectra taken as a whole, we can still seek improvements in χ^2_ν in those quality 1 and 2 observations for which the fit to the simple model can be rejected at the 90 percent confidence level. This is done by adding fitting parameters to the model spectra. In order to reject the simple model with 58 degrees of freedom, χ^2_ν must be larger than 1.25. There are only 3 quality 1 and 2 observations for which this is the case: the second NGC 7469 observation and the first and fifth 3C 120 observations.

The three modifications to the simple power law plus absorption model we have made in an attempt to better characterize the spectra of these three observations are not completely arbitrary; they correspond to effects we might expect to see in the soft X-ray spectrum of an AGN. They are the addition of i) a second, steeper power law (a "soft excess"), ii) a second absorbing column with $N_H \gtrsim 10^{22}$ cm^{-3} (a "partial covering") and iii) a Raymond-Smith

thermal plasma model (Raymond and Smith 1977, 1979), redshifted to the rest frame of the AGN.

A preferred modification of the simple power law model exists for each of the three observations. For the NGC 7469 observation, the addition of a second power law component produced a marginally significant improvement: although the F-test suggests this model is preferred at the 90% percent confidence level, the 67 percent confidence bounds on the flux from the second component includes zero. The inclusion of a redshifted Raymond-Smith plasma provided substantially improved fits for both 3C 120 observations; using the F-test, we find that in both cases the simple power law model is excluded with better than 98 percent confidence.

The existence of a preferred multicomponent model in each instance above raises the possibility that the fits to many more of the quality 1 and 2 spectra may be similarly improved by the addition of parameters. We have therefore applied the three modifications described above to all the other quality 1 and 2 observations (for which acceptable single power law models do exist). In only one instance out of 19 does a multicomponent model reduce χ^2 such that the F-test prefers it at a confidence level exceeding 90 percent (Fairall 9, Obs. 2; with a partial covering model). As with the NGC 7469 model above, however, the 67 percent confidence bounds for the flux of the second component includes zero. Since we expect two of the 22 quality 1 and 2 observations to have spectra which will be improved at the 90 percent level by the addition of components, we conclude that the only spectra for which strong evidence of a second component exists are those of 3C 120.

The existence of thermal line emission in the 3C 120 spectrum in this data has been previously suggested by Holt (1979); however, Holt reported only on Observation 1, and he fit a collection of discrete lines to the spectrum

rather than a composite Raymond-Smith model. For both observations, the best fit temperature is ~ 1 keV and the thermal component represents 10-20 percent of the 0.75-4.5 keV flux in a narrow band around 1 keV. The required volume emission measure of thermal gas is ~ 2 x 10^{66} cm^{-3} (assuming H_0 = 50 km s^{-1} Mpc^{-1}); this is a factor of ~ 10-1000 higher than what one might expect on the basis of typically quoted values of the radius (10^{17} cm) and density (10^6-10^7 cm^{-3}) of the intercloud gas in the broad line region of an AGN (Krolik and London 1983; Davidson and Netzer 1979, and references therein), the most likely source of thermal X-rays. If we are truly detecting thermal line emission from 3C 120, then either the broad line region is larger and/or denser than expected, or the emission arises elsewhere in the galaxy.

IV. The Soft X-Ray Properties of the High X-Ray Luminosity AGN

As can be seen from Table 2 and the discussion above, the best characterization of the 0.75-4.5 keV spectra of our sample of high X-ray luminosity AGN is a single power law plus a small amount of absorption. Only in one source does a strong suggestion of spectral features appear. We now discuss the X-ray properties of these AGN collectively and compare them to other X-ray measurements.

a. Spectral Index

A histogram of our inferred α for all the observations is shown in Figure 3. The various degrees of shading indicate where in the histogram the different quality observations fall; note the tendency of the poorest quality data to contribute lower α values to the sample. The mean value of α for all our observations is 0.66±0.36. We find the same mean α if we instead average by source. This $\langle\alpha\rangle$ is consistent with the $\langle\alpha\rangle$ values for X-ray emitting Seyferts type I and NELG's in the 2-40 keV band (Mushotzky et al. 1980; Mushotzky 1982,1983), for 50 Seyfert galaxies and quasars observed by the

Einstein MPC in the 1.5-10 keV band (Halpern 1982), and for the 2-165 keV spectra of 12 AGN (Rothschild et al. 1983). As can be seen by the size of the typical error depicted in Figure 3, much of the spread in α may be due to measurement error. There is also no inconsistency in the larger variance compared to that found by Mushotzky (1982, 1983) using HEAO-1 A2: the A2 spectra are deeper exposures with a larger detector and contain more than 5 times the number of counts in a typical SSS spectrum. We therefore believe that, with certain exceptions like 3C 273 and ESO 141-G55, the intrinsic spread in α among AGN may be quite small (see Rothschild et al. for a similar discussion and conclusion).

In addition to comparing the ensemble properties of our sample with those from other instruments, we may compare our values of α on a source-by-source basis with those from HEAO-1 A2 and on an observation-by-observation basis with those from the Einstein MPC. Such comparisons are made in Table 3, which contains the inferred spectral indices from each instrument, and in Figures 4a and 4b, in which the HEAO-1 A2 and the MPC values are plotted against the SSS values. Except for 3C 382 and ESO 141-G55[4], the SSS values are consistent

---

[4]Recent work (Tennant 1983) has shown that the variable soft excess in ESO 141-G55 reported by Mushotzky et al. (1980) is not associated with the active galaxy. We have used a single power law model with = 0.8 for the HEAO-1 data.

---

with those of HEAO-1 A2. While the allowed ranges of α from the MPC and the SSS are generally consistent, the majority of MPC best fit values are slightly larger than the SSS values. This is most likely due to some unknown systematic uncertainty and is a small effect which does not influence our

conclusions regarding the entire sample. We conclude that both collectively and individually the spectral indices of the high X-ray luminosity AGN show no variation from 0.75 to above 100 keV.

B. Absorption

Since the SSS bandpass extends below that of either the MPC or the A2 MED, it is more sensitive to low-energy absorption. Given the flat spectrum typical of AGN and the average data quality in our sample, the SSS allows measurement of the total column density (galactic plus intrinsic) as low as $\sim 2 \times 10^{21}$ cm^{-2}, about a factor of five lower than the MPC or the HEAO-1 MED. Although there are some sources for which the formal upper limit on N_H is well below this value (e.g. NRAO 140--see Table 1) and there are some spectra whose quality might allow a more stringent upper bound on N_H (e.g. IC 4329A or 3C 273), we will use 2×10^{21} cm^{-2} as a mean sensitivity for all sources because it is representative of our sample as a whole.

In Figure 5, we plot the best fit N_H values (with their formal error ranges from Table 1) against the galactic N_H in the line of sight (Burstein and Heiles 1982). In the case of Q0241+622, we use $N_H = 8.8 \times 10^{21}$ cm^{-2}, obtained from 21 cm measurements in the direction of the quasar (Margon and Kwitter 1978). In Figure 6 we plot a histogram of the differences between the SSS N_H value and the galactic N_H; a positive value represents the amount of absorbing material intrinsic to a source. From these two figures it is quite apparent that, aside from IC 4329A, we find no evidence of absorbing gas intrinsic to the high X-ray luminosity AGN with an upper limit of 2×10^{21} cm^{-2}. It should be noted that intrinsic absorption effects will not be masked by redshift for this group of AGN: the redshifts for all are less than 0.04, with the exceptions 3C 273 ($z = 0.15$) and NRAO 140 ($z = 1.25$).

C. Covering Fraction

Although our spectral modelling of the SSS data from high X-ray luminosity AGN favors a simple power law plus absorption, we cannot rule out models which include some small contribution from other spectral components. It is of interest to systematically place upper limits on the possible contribution of some of these. We are primarily interested in components whose existence is expected either on theoretical grounds or on the basis of their presence in other AGN spectra.

One component for which we can use our data to place upper limits is the partial covering of the X-ray source by "cold" ($T \sim 10^4$ K) clouds in the line of sight with $N_H \gtrsim 1 \times 10^{22}$ cm^{-2}. Such partial covering has been observed by the SSS in NGC 4151 (Holt et al. 1980), as well as in some other low luminosity AGN (Reichert et al. 1983). Also, theoretical models of the broadline region in AGN generally require column densities of this order of magnitude (Kwan and Krolik 1979, 1981). High partial covering (> 90 percent) by thick clouds is highly unlikely in the high X-ray luminosity AGN: if it is present, positive column densities would have been suggested by the HEAO-1 A2 MED, which was sensitive to column densities $\gtrsim 10^{22}$ cm^{-2} for mostly covered sources.

To place upper limits on the covering fraction in the quality 1 and 2 observations, we have systematically added into our spectral model increasing amounts of a second absorbed component until χ^2 increased by 6 from its mimimum value. The value of α has been allowed to vary within the range allowed by the single power law fits. The maximum allowed value of N_H varies from observation to observation; for a given observation, it was determined from the upper limit on the optical depths of the absorption edges of Mg, Si, and S, assuming normal cosmic abundances. The upper limits on the covering

fraction are compiled in Table 4, along with the maximum value of N_H allowed. The mean upper limit on the covering fraction is 0.52±0.15, with individual limits ranging from 0.25 to 0.78. For the quality 1 observations the average is 0.40±0.11, for the quality 2 observation it is 0.63±0.10; the upper limit on the covered fraction increases with decreasing data quality. We conclude that the high X-ray luminosity AGN are mostly or fully uncovered, in contrast to the AGN with lower X-ray luminosity (Reichert et al. 1983; Mushotzky 1982; Lawrence and Elvis 1982).

One special case exists in our data: IC 4329A, whose absorption column greatly exceeds the galactic value. The absorption measured in the X-ray band is consistent with the optical interstellar absorption in this galaxy (Wilson and Penston 1979). This suggests that the IC 4329A nucleus is fully covered; the low N_H ($<10^{22}$ cm^{-2}) suggests this covering is produced by material external to the active region. If this is so, then this represents the first measurement of the column density of the interstellar medium in another galaxy. Two tests for partial covering are possible in IC 4329A. First, we assume the measured N_H is from outside the active region (i.e., associated with the main body of the galaxy), and place a limit on the fraction of additional, high column density ($N_H > 10^{22}$ cm^{-2}) gas allowed. This is similar to the approach taken for all the other AGN; the result (covering fraction less than 0.42) is contained in Table 4. The second test places an upper limit on the "uncovered" fraction of the nucleus; we systematically add a higher percentage of covering by material with only the (local) galactic column density. The upper limit on the uncovered fraction found in this way is 9 percent. Moreover, the largest allowed value of N_H of the covered fraction is 8×10^{21} cm^{-2}, supporting the inference * we are observing covering from a site other than the active region.

D. Fluxes and Variability

The SSS counting rates from these sources are too low to permit a search for variability on short time scales (less than an observation length) as can be performed by instruments with larger collecting areas (see, e.g., Tennant and Mushotzky 1983). On the other hand, we believe the quality of the data do allow, if reasonable caution is exercised, searches for flux (and model parameter) variations over time scales between observations (1-200 days). Because of the effects of systematics on the total count rate in the SSS, any given flux measurement is probably accurate to no more than 10 percent. Therefore, flux variations are to be believed only if the ratio of the change in flux to the average flux $|\Delta f/\bar{f}|$ is at least as large as 20 percent.

We can also compare the SSS flux for each source with the flux measured simultaneously by the MPC and at other times by HEAO-1 A2. Despite the general consistency between the spectral indices inferred from the SSS, the MPC and the HEAO-1 data, inferring the flux in one band by extrapolating the spectrum measured in another is inherently less reliable than is a direct comparison at a common energy value. As a basis for flux comparison we therefore use f_3, the flux in a 1 keV band centered at 3 keV. This spectral band is common in all three instruments.

In Table 5 we list the values of f_3 of the observed AGN as measured by the SSS, the MPC and the HEAO-1 A2. For each SSS observation we also list the inferred flux within the instrumental bandpass (0.75-4.5 keV) corrected for galactic absorption. For most of these observations, the 2-10 keV MPC flux, and hence f_3, is also uncertain by 10 percent due to systematic effects (Halpern 1982, Tennant 1983). The HEAO-1 A2 fluxes are uncertain by $\sim$ 10 percent due to fluctuations in the X-ray background (Tennant and Mushotzky 1983). The SSS fluxes and the MPC fluxes at 3 keV are generally consistent at

the 20 percent level. In addition, both the SSS and MPC fluxes tend to be consistent with the A2 fluxes at 3 keV, suggesting that, in general, the flux of a high X-ray luminosity AGN is weakly variable, showing flux variations of no more than 30 percent (typically) over a time scale of > 1 year. There are only a few indications of large amplitude variability ($|\Delta f_3/f_3| > 1$) on this timescale: III Zw 2, QO241+622, 3C 273, and IC 4329A.

Returning to the question of flux variability among SSS observations, we find that of the six sources observed multiply, two are definitely variable ($|\Delta f_3/\bar{f}_3| > 20$ percent) and two show evidence of variability ($|\Delta f_3/\bar{f}_3| \sim 20$ percent). For the two variable sources, 3C 273 and 3C 120, the sense and the magnitude of the flux changes as detected by the MPC are consistent with the SSS variability (~ 50 percent increase in flux over 200 days in 3C 273; 70 percent decrease in 182 days, followed by a 6 percent increase in 15 days in 3C 120). This is also the case for the two marginally variable sources, Mkn 509 and NGC 7469.

The only source displaying any real evidence of spectral variability is 3C 120, for which α varies from 1 to 0.2 and back to 1 over 200 days. This source is thus unique in our sample in its both spectral properties and its temporal behavior. A discussion of the physics involved in the variability of spectral shape, and in the appearance of X-ray line emission, is beyond the scope of the present publication.

E. Correlations with Luminosity and Spectral Index

In Table 6, we have listed the AGN in our sample in decreasing order by $\langle L_{SSS} \rangle$, their average intrinsic (i.e. absorption removed) 0.75-4.5 keV luminosity. In order to discuss possible correlations between the soft X-ray spectral index and luminosity and quantities inferred from measurements in other bands, we have included $\langle L_{SSS} \rangle$ along with the average spectral

index $\langle\alpha_{sss}\rangle$, as well as values of log($\nu L\nu$) representative of three wavebands (3 keV - X-ray; 1450 A - ultraviolet; 3.5 μm - infrared) and the luminosities in two lines, Hβ and [O III]. The line and 3.5 μm luminosities are taken from the compilation of Lawrence and Elvis (1982); the 1450 A luminosities are taken from Wu, Boggess and Gull (1983) except for 3C 273 (Ulrich et al. 1980). Use of νL_ν as opposed to L_ν permits a more straightforward comparison of relative power radiated in each band. All luminosities have been calculated assuming an H_0 of 50 km s^{-1} Mpc^{-1} (Lawrence and Elvis 1982; Wu, Boggess and Gull 1982). The final column in Table 6 contains the measured slopes of the ultraviolet nonthermal continuum (Malkan and Sargent 1982).

It has been established that a strong correlation exists between the 2-10 keV luminosity and all the non-X-ray band quantities in Table 6 (Lawrence and Elvis 1982; Wu, Boggess and Gull 1983). Since our SSS measurements of the high X-ray luminosity AGN have demonstrated that the 0.75-4.5 spectrum is simply an extension of the 2-10 keV spectral behavior, it is clear that $\langle L_{sss}\rangle$ will also correlate with all of these quantities.

In Figure 7 we have plotted $\langle L_{sss}\rangle$ versus $\langle\alpha_{sss}\rangle$. The solid vertical line in Figure 7 represents the mean α above 2 keV; the flanking dashed lines represent the dispersion about this mean. Over the 3.5 orders of magnitude in luminosity covered by our sample, $\langle\alpha_{sss}\rangle$ and $\langle L_{sss}\rangle$ are independent of one another; the probability of a correlation is less than 40 percent. If we consider the twelve Seyferts (closed circles) or the three quasars independently, we find no real evidence of a $\langle\alpha_{sss}\rangle$-$\langle L_{sss}\rangle$ correlation in either subset (the probability in each case is less than 40 percent), nor do we find a systematic difference in $\langle\alpha_{sss}\rangle$ between Seyferts and quasars. This suggests that the mechanism producing the X-rays in AGN is independent of the production rate across three and one half orders of magnitude in luminosity

and independent of AGN type. This luminosity independence of spectral shape has been noted by Mushotzky (1983), whose observations cover a different luminosity band ($10^{42.5} < L_X < 10^{45}$ erg s^{-1}) at somewhat higher energies (2-20 keV). With the inclusion of NRAO 140, we have extended by an order of magnitude the range of X-ray luminosities over which the independence of spectral shape has been observed.

Since the quantities Hβ, OIII, $L_{3.5}$ and L_{1450} all scale with $\langle L_{SSS} \rangle$, we can conclude that all these quanties are also approximately independent of the spectral shape in the X-ray band.

V. DISCUSSION

A. The Universal Spectral Shape

One of our most striking results is the simplicity with which it is possible to describe the X-ray continua of these active galactic nuclei. The mean spectral indices over the photon energy range 0.5-60 keV are all approximately the same: $(\alpha_{SSS}) \simeq (\alpha_{MPC}) \simeq (\alpha_{HEAO-1}) \simeq 0.7$ (this paper; Halpern 1982; Mushotzky et al. 1980). Moreover, the scatter in the spectral indices is small, $\lesssim \pm 0.35$. This universality of spectrum is made even more striking by the fact that very similarly-shaped spectra are seen in a wide variety of other observations: the radio continua of spiral galaxies, classical double radio sources, supernova remnants, etc. Several conclusions follow from our finding that the X-ray spectra of active galactic nuclei follow this "universal" power-law (Rothschild et al. 1983).

First, the smoothness of the X-ray spectrum of active galaxies over a range of two orders of magnitude in photon energy suggests that whatever mechanism produces the X-ray photons has no special energy scale over a very broad range. Meszaros (1983) has pointed out that optically thin bremsstrahlung from plasma whose emission measure per temperature is inversely

proportional to temperature (as would be produced, for example, by spherical free-fall in which the temperature scales inversely with radius) produces a spectrum with spectral index roughly 0.6-0.7 over essentially the entire range of photon energies between the minimum and maximum temperatures. Models of this class, in which a wide range of temperatures contribute, can be consistent with the observed X-ray spectra.

Similarly, some, but not all, nonthermal mechanisms may be able to produce spectra such as these. Synchrotron-based models (with or without Comptonization: e.g. Mushotzky 1977) yield power-law spectra, but they require electron acceleration mechanisms which produce the right electron distribution function. Non-relativistic Comptonization models (e.g. Katz 1976) may also be able to account for the soft end of the spectrum, but the diffusion approximation which lies behind them breaks down when the spectrum extends up to photon energies greater than $\sim 0.1\ m_e c^2$.

Second, the spectrum of active galaxies does not match the spectrum of the cosmic X-ray background. The measured spectrum of the cosmic background in the photon energy range from 3 keV to 60 keV is very well fit by thermal bremsstrahlung at a temperature of 40 keV, so that the spectral index from 3 keV to $\sim$ 30 keV is $\simeq$ 0.4 (Marshall et al. 1980). It is customary to assume that this spectrum extrapolates smoothly down to 0.5 keV; actual measurements are made difficult by local galactic emission and absorption. If we share this assumption, it is clear that the narrowness of the distribution of spectral shapes in our sample precludes an origin for the cosmic X-ray background in galaxies of this type (DeZotti et al. 1982).

All but three of the objects in our sample are Seyfert galaxies, rather than quasars, so it remains possible that the quasars which are widely regarded as generating a large fraction of the few keV X-ray background

(Zamorani et al. 1981; Avni and Tananbaum 1982) may have a different mean spectrum. All that it is possible to say at this point is that the three quasars in our sample do not demand this possibility.

One important issue concerning the shape of the continuum spectrum which has not been resolved by our results is the value of the energy at which the X-ray slope α_{sss} connects with the slope as measured in the ultraviolet α_{uv}. As reported in Malkan and Sargent (1982) and Wu, Boggess and Gull (1983), a naive extrapolation of the shape of the UV continuum out to the X-ray band results in the two spectra intersecting somewhere between 0.5 and 2 keV. If this were the case, our SSS observations would have required a second, steeper power law component in addition to the power law consistent with that at higher energies. Stated more clearly, the SSS observations would have required a "soft excess". The fact that our observations require no such soft excess means that the UV and X-ray slopes join at some energy less than 0.75 keV. On the basis of the Malkan and Sargent results, we can infer that the X-ray and UV slopes do not join smoothly; between 1000 A (~ 12 eV) and 750 eV, the continuum spectrum must experience a sharp turnover which links the UV continuum slope to the X-ray slope.

B. The Lack of Soft X-Ray Absorption

We have found that, with one exception (IC 4329A), luminous Seyfert galaxies and quasars exhibit little or no intrinsic soft X-ray absorption. In this section we will examine the implications of our measurements for each of three possible sites of X-ray opacity: the broad emission-line region immediately surrounding the source of the X-ray emission; the narrow emission-line region, typically 100-1000 times farther away; and the intergalactic medium. As sensitive as they are, our measurements say little of interest about the interstellar medium of the parent galaxy; a further

increase in sensitivity by a factor of three or so would be necessary before it would be possible to detect column densities of the magnitude typically observed along axial lines of sight to the centers of spiral galaxies.

i. The broad emission-line region

The generally accepted view of the broad emission-line region in Type 1 Seyfert galaxies and quasars is that it is a volume of radius $\simeq 0.05\ (L_{ion}/10^{44}\ \mathrm{erg\ s^{-1}})^{1/2}$ pc (L_{ion} is the ionizing luminosity, i.e. the portion between 1 and 1000 Rydbergs), filled primarily by a very hot, rather rarefied plasma within which a large number of very small ($\sim 10^{13}$ cm), dense ($\sim 10^{9}$ - 10^{10} $\mathrm{cm^{-3}}$), cool ($\simeq 10^{4}$ K) clouds are embedded in rough pressure equilibrium (Davidson and Netzer 1979; Krolik, McKee, and Tarter 1981). The hydrogen nucleus column density across this region due to the hot intercloud medium alone is approximately:

$$N_H \simeq 1.3 \times 10^{23} \left(\frac{\tilde{p}_h}{\tilde{p}_c}\right) T_{h8}^{-1} \left(\frac{\tilde{p}_{c,13} L_{ion,44}}{8\Xi}\right)^{1/2} \mathrm{cm^{-2}}, \qquad (1)$$

where $\tilde{p}$ is the pressure in units of K $\mathrm{cm^{-3}}$, subscripts h and c refer respectively to the hot intercloud medium and the cool clouds, $\tilde{p}_{c,13}$ is the cloud pressure in units of 10^{13} K $\mathrm{cm^{-3}}$, T_{h8} is the temperature of the hot medium in units of 10^{8} K, $L_{ion,44}$ is L_{ion} in units of 10^{44} erg $\mathrm{s^{-1}}$, and Ξ is the radiation pressure to gas pressure ratio (Krolik, McKee, and Tarter 1981). If this hot intercloud medium were not mostly ionized, our measurements would be in clear contradiction with this standard picture.

However, under such conditions of strong photoionization and high temperature, oxygen (which makes the single largest contribution to the opacity in the range from 0.8 - 3 keV: Morrison and McCammon 1983) is almost entirely stripped of electrons. Making the approximation that all oxygen

nuclei have at most one electron remaining, we find that the ratio of O^{+7} to O^{+8} number density is:

$$\frac{n(O^{+7})}{n(O^{+8})} \simeq \frac{2.1 \times 10^{-4}\ T_{h8}^{-1.18}}{\Xi\ T_{h8}^{1/2}\ F_X/F_{ion} + 0.16\ \exp[0.10(1-1/T_{h8})/(1+2.5T_{h8})]} \qquad (2)$$

under conditions of ionization equilibrium, but not necessarily radiative equilibrium (i.e. the temperature may be determined by other processes than radiative heating and cooling: see Krolik, McKee, and Tarter 1981 and Krolik and London 1983 for examples). The quantity F_X is the flux from the oxygen edge (0.87 keV) to 500 keV; F_{ion} is the ionizing flux from 1 to 10^3 Rydberg. For typical Seyfert galaxy and quasar spectra, $F_X/F_{ion} \simeq 1 - 2$ (Rothschild et al. 1983 for X-ray spectra; Wu, Boggess, and Gull 1983 for UV spectra). Studies of the line-emitting properties of the clouds have shown that $0.3 < \Xi < 2$ (Kwan and Krolik 1981); photoionization dominates collisional ionization in these circumstances. Combining Eqs. 1 and 2 then gives a lower limit on the temperature of the hot intercloud medium:

$$T_{h8} > 0.26\ \Xi^{-0.56} \left(\frac{\tilde{P}_{c,13}\ L_{ion,44}}{8}\right)^{0.19} \left(\frac{F_{ion}}{F_X}\frac{\tilde{P}_h}{\tilde{P}_c}\ N_{abs,21}^{-1}\right)^{0.37} \qquad (3)$$

where N_{abs} is the upper limit on the equivalent hydrogen column density in units of 10^{21} cm^{-2}. Note that the two orders of magnitude greater luminosity found in quasars than Seyferts only raises this lower limit by about a factor of two.

In some theoretical models of quasar accretion (Shields and McKee 1981; Krolik and London 1983), the temperature of the hot intercloud medium can be as low as $\sim 10^7$ K (depending on the free parameters of the model). Thus, the lower limit from the SSS data provides a significant constraint on models of

the hot intercloud medium, typically $T_{h8} \gtrsim 0.3$ for Seyferts and $T_{h8} \gtrsim 0.8$ for quasars.

It is also possible that one of the cool clouds may obscure the source of X-rays. If a cloud were to lie along the line of sight to the X-ray source, it would present an optical depth in partially-ionized oxygen equivalent to at least 10^{22} cm^{-2} (Kwan and Krolik 1979), but it is an open question whether a single such cloud is large enough to cover the entire source. If this is so, and if we assume that the apriori probability distribution for the cloud covering fraction is uniform over the interval 0-1, then we conclude from the fact that a broad-line cloud covers the source in none of our fifteen observations that at the 90 percent confidence level the mean covering fraction is less than 15 percent.

If the clouds are individually too small to cover the X-ray source, the first column of Table IV presents our upper limits on covering fractions. The second column of Table IV gives the covering fraction predicted by comparing the Hβ luminosity L(Hβ) to the observed ionizing luminosity:

$$C = 0.15 \left(\frac{L(H\beta)/L_{ion}}{0.01}\right) \left(\frac{\tilde{P}_{c,13^{\Xi}}}{8}\right) \left(\frac{A_{rad}/A_{cs}}{4}\right) \qquad (4)$$

where we have used the Hβ emissivity per unit area computed by Kwan and Krolik (1981). A_{rad}/A_{cs} is the ratio of the clouds' radiating surface areas to their cross sections, while L_{ion} is calculated by assigning a power-law index of -2 to the ultraviolet spectrum from 1450 A to the soft X-ray regime, and extrapolating the observed X-ray spectrum to 13.6 keV. The figures in Table IV are computed with all the scaling factors of Eq. 4 set equal to unity. The covering fraction predicted by the Hβ luminosity for one object, MCG 2-58-22, is almost exactly equal to our upper limit for that object, but all the other

predicted covering fractions are rather smaller than the upper limits. Because the model parameters ($\tilde{\rho}_{c,13}$, Ξ, the cloud column density, A_{rad}/A_{cs}, and the continuum shape) and the model calculations (because of approximations, uncertainty in the atomic data, etc.) are uncertain by at least factors of two, there would only be a real contradiction if the predicted covering fraction exceeded the upper limits by an order of magnitude or more.

Previous workers have suggested that there is a tendency for the less-luminous Seyfert galaxies to have greater covering fractions (Holt et al. 1980; Mushotzky 1982; Lawrence and Elvis 1982). There is no such correlation in our data, either in the covering fractions predicted from the ratio $L(H\beta)/L_{ion}$ or in the upper limits derived from the lack of soft X-ray absorption. These findings may not be inconsistent, due to the narrower range of luminosities covered by our sample than by the others.

ii. The narrow emission-line region

a. Gas column density

The generally accepted picture of the narrow emission-line region is qualitatively similar to that of the broad line region, but the densities are lower, the distances are larger, and the physical conditions in general are known in less detail. The radius is thought to be $\sim 30\ L_{ion,44}^{1/2}$ pc, the internal cloud densities around 10^4 cm^{-3}, and the individual cloud column densities $\sim$ several $\times\ 10^{21}$ cm^{-2} (Ferland 1981, Ferland and Mushotzky 1982). The predicted column density of hot gas in the narrow line region is 10 - 1000 times smaller than in the broad line region, so the lower limit on the temperature is about 10 times weaker:

$$T_{h8} > 0.022\ \Xi^{-0.56}\ \left(\frac{\tilde{\rho}_{c,8} L_{ion,44}}{2}\right)^{0.19} \left(\frac{F_{ion}}{F_x}\ \frac{\tilde{\rho}_h}{\tilde{\rho}_c}\ N_{abs,21}^{-1}\right)^{0.37}, \qquad (5)$$

where $\tilde{P}_{c,8}$ is the narrow line cloud pressure in units of 10^8 K cm^{-3}, and $N_{abs,21}$ is the column density in the narrow line region in units of 10^{21} cm^{-2}. From (5) we find that at $L_{ion} \sim 10^{44}$ erg/sec, $T_{h8} \gtrsim .03$ for the intercloud medium in the narrow line region.

Provided that the column density of the narrow line clouds is really at least 10^{21} cm^{-2}, the arguments giving limits on cloud covering fraction carry through for the narrow line clouds just as for the broad line clouds, so we will not repeat them here.

b. Dust

One aspect of the narrow line region does differ from the broad line region, however. A number of workers have proposed, for diverse reasons, that there is a significant dust content in the narrow line region. If the standard dust to gas ratio found in our galaxy applies to Seyfert galaxies, a column density of 2×10^{21} A_V cm^{-2} would be implied (Gorenstein 1975; Ryter, Cesarsky, and Audouze 1975). Even if Seyfert galaxies have no oxygen in the gas phase that retains any electrons, the oxygen in the dust would still present an equivalent absorbing column density of 1×10^{21} A_V cm^{-2} so long as its chemical composition (silicates and water ice in addition to graphite) and size distribution were the same as in our galaxy (Fireman 1974; Mathis, Rumpl, and Nordsieck 1977). Our upper limits of $\sim 2 \times 10^{21}$ cm^{-2} on the effective hydrogen column density therefore pose an upper limit on A_V of $\sim 0.5 - 1$, with the larger value applying when the only unstripped oxygen in the line of sight is in dust grains. As we shall discuss, certain arguments for dust are consistent with these upper limits, while others are in marginal contradiction.

Rieke (1978) proposed that the 10μ radiation he observed from Seyfert

galaxies was due to thermal emission by dust. It is possible to compare the amount of dust required with our upper limits by the following argument. Suppose that the infrared flux is defined to be $\nu F_\nu(10\mu)$ and the ultraviolet flux available for reradiation is $\nu F_\nu(1450A)$. Then the ratio of infrared to ultraviolet flux is:

$$\frac{F_{ir}}{F_{uv}} = [\exp(\tau_{1450}) - 1]^{-1} \qquad (6)$$

where τ_{1450} is the dust absorption optical depth at 1450 A. Using the data presented by Rieke (1978) and Wu, Boggess, and Gull (1983), it is then possible to find τ_{1450} for five Seyfert galaxies from our sample (III Zw 2, 3C 120, Mkn 509, NGC 7469, and NGC 5548). The reddening curve given by Savage and Mathis (1979) provides a conversion to E(B-V), and a standard R factor ($\approx$ 3 - 3.3) converts the result to A_V. Following this procedure, we find that it is possible for these five galaxies to generate their 10μ flux by reradiation from dust, for the implied A_V's never exceed $\sim$ 0.6. The corresponding τ_{1450} never exceeds 1.5. If the infrared flux is significantly larger than $\nu F_\nu(10\mu)$, the required dust extinction will be in conflict with our upper limits.

Another argument for a similar amount of dust in the narrow line region has been given by Netzer and Davidson (1979). In order to account for several broad-line ratios that are redder than would conventionally be expected, they suggested that $A_V \approx 0.6$. Given the minimal conversion between dust reddening and absorbing column density, this much dust would be permitted in most of our galaxies (including, of course, the ones listed in the previous paragraph), but would be marginally ruled out in Fairall 9, NRAO 140, and 3C 273.

Finally, high-resolution studies of the narrow line profiles (Vrtilek

1983) have shown that their characteristic asymmetry suggests a dust optical depth at 5000 A of roughly unity. Again, following the minimal conversion from dust reddening to absorbing column density, $A_V = 1$ is marginally consistent with all but one of our observations, and consistent with the IC 4329A observation.

iii. The intergalactic medium

It is unknown whether the intergalactic medium contains any significant abundance of heavy elements. Various theoretical proposals have been made in which an early generation of stars (Population III) contaminates the primordial hydrogen/helium mix of the universe with heavier elements (Rees 1978ab; Hartquist and Cameron 1977), or merged supernova explosions in young galaxies eject processed material into the intergalactic medium (Bookbinder et al. 1980; Ostriker and Cowie 1981). If the intergalactic medium has a density near closure, possesses close to a solar abundance of oxygen, and is not too hot, then it should present a significant opacity to soft X-rays that traverse cosmological distances (Shapiro and Bahcall 1980).

Our best data on a distant object is for 3C 273, in which the upper bound of effective hydrogen column density (i.e. unstripped oxygen column density scaled by the solar abundance of oxygen) is $\simeq 2 \times 10^{21}$ cm^{-2}. This limit may be interpreted as either an upper limit on the density of oxygen at fixed temperature (which may be more conveniently expressed by the product of oxygen abundance and gas density relative to closure), or as a lower limit on the temperature of the intergalactic medium. An approximate calculation (which takes no account of the redshift of 3C 273 in distorting the energy-dependence of the oxygen-edge opacity) gives the following expression for the effective hydrogen column density to 3C 273:

$$N_{eff}(3C\ 273) \simeq 7.5 \times 10^{18}\ T_{IGM,8}^{-1.176}\ (1 + 2.47\ T_{IGM,8}) \qquad (7)$$
$$\times\ \exp[0.10(1/T_{IGM,8} - 1)]h\Omega\ X(0)/X_o(0)\ cm^{-2}$$

where $T_{IGM,8}$ is the temperature of the intergalactic medium in units of 10^8 K, h is the Hubble constant in units of 50 km s^{-1} Mpc^{-1}, Ω is the density relative to closure, X(0) is the oxygen abundance relative to hydrogen, and we have assumed both collisional ionization equilibrium and that all oxygen is either O^{+7} or O^{+8}. Eq. 8 gives, for example, an upper limit to $h\Omega X(0)/X_o(0)$ of $\simeq 6$ for $T_{IGM} = 10^7$ K, or a lower limit to the temperature of 5×10^6 K for $h\Omega X(0)/X_o(0) = 1$.

VI. SUMMARY AND CONCLUSIONS

We have presented the results of fitting 28 Einstein SSS spectra of 15 AGN whose 2-10 keV luminosities exceed 3×10^{43} erg s^{-1}. We have found the following:

1. The spectra are consistent with a single power law plus absorption. The average spectral index is 0.66±0.36, consistent with that inferred from simultaneous MPC measurements and earlier HEAO-1 A2 measurements. For all but one AGN, we find an upper limit on the intrinsic column density of 2×10^{21} cm^{-2}.

2. We place upper limits on the fraction of each AGN covered by material with $N_H > 10^{22}$ cm^{-2} (i.e., broad line clouds) in the range 0.2-0.8, with an average of 0.5.

3. We find that, in general, the flux of a high X-ray luminosity AGN is weakly variable, showing variations of typically 30 percent on a time scale of greater than 1 year. Of six objects observed more than once by the SSS, only 3C 273 and 3C 120 show variations greater than 50 percent about their average flux on time scales less than 200 days. Only 3C 120 shows any suggestion of

variability of its spectral parameters.

4. The spectral indices of these AGN are uncorrelated with their 0.75-4.5 keV luminosities, over the luminosity range $43.5 < \log (L_{sss}) < 47$. This suggests that the X-ray production mechanism is independent of the production rate over 3.5 orders of magnitude in luminosity.

5. Down to 0.75 keV, we observe no evidence of a "soft excess". This indicates that the UV spectrum must steepen between 13.6 and 500 eV.

6. The upper limit on the intrinsic column density allows us to place meaningful lower limits on the temperature of the intercloud medium in both the broad line region ($T > 2.6 \times 10^7$ K) and the narrow line region (2.2×10^6 K), and of the intergalactic medium.

ACKNOWLEDGMENTS

The authors wish to acknowledge helpful discussions with J. Halpern, G. Ferland, T. Kallman, G. Reichert and J. Kriss. We also thank P. Hertz for performing the K-S test on our data. We thank A. Szymkowiak and J. Swank for assistance with the data analysis and modeling the galactic absorption. J.K. extends his gratitude to Dr. F.B. McDonald for the hospitality extended during his visit to GSFC while this work was being performed.

REFERENCES

Apparao, K.M.V., Bignami, G.F., Maraschi, L., Helmken, H., Margon, B., Hjellming, R., Bradt, H.V., and Dower, R.G. 1978, Nature, 273, 450.

Avni, Y., and Tananbaum, H. 2982, Ap. J. 262, L17.

Bookbinder, J., Cowie, L.L., Krolik, J.H., Ostriker, J.P., and Rees, M.J. 1980, Ap. J. 237, 647.

Bowyer, C.S., Lampton, M., Mack, J., and de Mendonca, F. 1970, Ap. J. (Letters), 161, L1.

Burstein, D., and Heiles, C. 1982, A.J., 87, 1165.

Davidson, K., and Netzer, H. 1979, Rev. Mod. Phys. 51, 715.

DeZotti G., Boldt, E.A., Cavaliere, A., Danese, L., Marshall, F., Swank, J., and Szymkowiak, A. 1982, Ap. J. 253, 47.

Elvis, M., Maccacaro, T., Wilson, A.S., Ward, M.J., Penston, M.V., Fosbury, R.A.E., and Perola, G. 1978, M.N.R.A.S., 183, 129.

Ferland, G., 1981, Ap. J. 249, 17.

Ferland, G., and Mushotzky, R. 1982, Ap. J. 262, 564.

Fireman, E.L. 1974, Ap. J. 187, 57.

Gorenstein, P. 1975, Ap. J. 198, 95.

Halpern, J.P. 1982, Ph.D. Thesis, Harvard University.

Hartquist, T.W., and Cameron, A.G.W. 1977, Astr. Sp. Sci. 48, 145.

Holt, S.S. 1979, in HEAO Science Symposium, held at MSFC, May 8-9, 1979, NASA CP-2113), 292.

Holt, S.S. 1981, in X-Ray Astronomy with the Einstein Satellite, ed. R. Giacconi (Dordrecht:Reidel), 173.

Holt, S.S., Mushotzky, R.F., Becker, R.H., Boldt, E.A., Serlemitsos, P.J., Szymkowiak, A.E., and White, N.E. 1980, Ap. J. (Letters), 241, L13.

Holt, S.S., White, N.E., Becker, R.H., Boldt, E.A., Mushotzky, R.F., Serlemitsos, P.J., and Smith, B.W. 1979, Ap. J. (Letters), 234, L65.

Joyce, R.M., Becker, R.H., Birsa, F.B., H olt, S.S., and Noordzy, M.P. 1978, IEEE Trans. Nucl. Sci. NS-25, 453.

Katz, J.I. 1976, Ap. J. 206, 910.

Krolik, J.H., McKee, C.F., and Tarter, C.B. 1981, Ap. J. 249, 422.

Krolik, J.H., and London, R.A. 1983, Ap. J. 267, 18.

Kwan, J.Y., and Krolik, J.H. 1979, Ap. J. (Letters) 233, L91.

Kwan, J.Y., and Krolik, J.H. 1981, Ap. J. 250, 478.

Lampton, M., Margon, B., and Bowyer, S. 1976, Ap. J. 208, 177.

Lawrence, A., and Elvis, M. 1982, Ap. J., 256, 410.

Malkan, M.A., and Sargent, W.L.W. 1982, Ap. J. 254, 22.

Margon, B., and Kwitter, K.B. 1978, Ap. J. (Letters), 224, L43.

Marshall, F.E., Boldt, E.A., Holt, S.S., Miller, R., Mushotzky, R.F., Rose, L.A., Rothschild, R.E., and Serlemitsos, P.J. 1980, Ap. J. 235, 4.

Marshall, F.E., Boldt, E.A., Holt, S.S., Mushotzky, R.F., Pravdo, S.H., Rothschild, R.E., and Serlemitsos, P.J. 1979, Ap. J. (Suppl.) 40, 657.

Mathis, J.S., Rumpl, W., and Nordsieck, K.H. 1977, Ap. J. 217, 425.

Meszaros, P. 1983, preprint.

Morrison, R. and McCammon, D. 1983, Ap. J. 270, 119.

Mushotzky, R.F. 1977, Nature 265, 225.

Mushotzky, R.F. 1982, Ap. J. 256, 92.

Mushotzky, R.F. 1983, Proceedings IAU/COSPAR Meeting on High Energy Astrophysics and Cosmology.

Mushotzky, R.F., Marshall, F.E., Boldt, E.A., Holt, S.S., and Serlemitsos, P.J. 1980, Ap. J., 235, 377.

Netzer, H., and Davidson, K. 1979, M.N.R.A.S. 187, 871.

Ostriker, J.P., and Cowie, L.L. 1981, Ap. J. (Letters) 243, L127.

Piccinotti, G., Mushotzky, R.F., Boldt, E.A., Holt, S.S., Marshall, F.E., Serlemitsos, P.J., and Shafer, R.A. 1982, Ap. J. 253, 485.

Raymond, J.C. and Smith, B.W. 1977, Ap. J. Suppl. 35, 419.

Raymond, J.C. and Smith, B.W. 1979, private communication.

Rees, M.J. 1978a, Phys. Scripta 17, 371.

Rees, M.J. 1978b, Nature 275, 35.

Reichert, G., Petre, R., Mushotzky, R., and Holt, S.S. 1983, B.A.A.S. 15, 675.

Rieke, G. 1978, Ap. J. 226, 550.

Rothschild, R., Mushotzky, R.F., Baity, W., Gruber, D., and Peterson, L.E. 1983, Ap. J. 269, 423.

Ryter, C., Cesarsky, C.J., and Audouze, J. 1975, Ap. J. 198, 103.

Savage, B.D., and Mathis, J.S. 1979, Ann. Rev. Astron. Astrop. 17, 73.

Shapiro, P.R., and Bahcall, J.N. 1980, Ap. J. 241, 1.

Shields, G.A., and McKee, C.F. 1981, Ap. J. (Letters) 246, L57.

Tananbaum, H., Peters, G., Forman, W., Giacconi, R., and Jones, C. 1978, Ap. J. 223, 74.

Tennant, A.F. 1983, Ph.D. Thesis, Univ. of Maryland.

Tennant, A.F., and Mushotzky, R.F. 1983, Ap. J., 264, 92.

Ulrich, M.H., Boksenberg, A., Bromage, G., Carswell, R., Elvius, A., Gabriel, A., Gondhalekar, P.M., Lind, J., Lindgren, L., Longair, M.S., Penston, M.V., Perryman, M.A.C., Peltini, M., Perola, G.C., Rees, M., Sciama, D., Snijders, M.A.J., Tanzi, E., Tarenghi, M., and Wilson, R. 1980, M.N.R.A.S. 192, 561.

Vrtilek, J. 1983, Ph.D. thesis, Harvard University.

Wilson, A., and Penston, M. 1979, Ap. J. 232, 389.

Worrall, D.M., Boldt, E.A., Holt, S.S., and Serlemitsos, P.J. 1980, Ap. J.,

240, 420.

Worrall, D.M., Mushotzky, R.F., Boldt, E.A., Holt, S.S., and Serlemitsos, P.J. 1979, Ap. J. 232, 683.

Wu, C.-C., Boggess, A., and Gull, T.R. 1983, Ap. J., 266, 28.

Zamorani, G., Henry, J.P., Maccacaro, T., Tananbaum, H., Soltan, A., Avni, Y., Liebert, J., Stocke, J., Strittmatter, P.A., Seymann, R.J., Smith, M.G., and Condon, J.J. 1981, Ap. J. 245, 357.

TABLE 1

SSS Observation Log - High Luminosity AGN

Source	r.a. h	r.a. m	r.a. s	dec °	dec ′	dec ″	Type	z	Obs. #	Day (of 1978)	Obs. Time (ks)	Data Quality
III Zw 2	00	07	57	10	41	48	Sey 1	0.090		539.7	5.98	2
Fairall 9	01	21	51	-59	04	00	Sey 1	0.046	1	495.2	3.73	2
									2	541.0	10.2	2
Q0241+622	02	41	01	62	15	27	QSO	0.044		397.6	7.21	3
NRAO 140	03	33	25	32	08	28	QSO	1.259		425.5	7.99	3
3C 111	04	15	01	37	54	20	Sey 1	0.049		426.2	3.15	3
3C 120	04	30	32	05	14	59	Sey 1	0.033	1	414.2	7.29	2
									2	435.3	7.78	2
									3	597.1	6.76	2
									4	598.1	4.42	2
									5	613.0	5.32	2
MCG 8-11-11	05	51	10	46	25	55	Sey 1	0.021		454.0	8.48	2
3C 273	12	26	33	02	19	43	QSO	0.158	1	346.6	9.34	2
									2	538.1	7.41	1
									3	539.1	7.33	1
									4	540.7	6.80	1
IC 4329A	13	46	28	-30	03	40	Sey 1	0.014		588.7	12.1	1
NGC 5548	14	15	43	25	22	00	Sey 1	0.017		382.1	2.51	3
3C 382	18	33	12	32	39	18	Sey 1	0.059		454.0	6.14	3
ESO 141-G55	19	16	57	-58	45	50	Sey 1	0.037		454.7	4.18	2
Mkn 509	20	41	26	-10	54	17	Sey 1	0.036	1	480.3	7.78	2
									2	496.6	3.48	2
									3	499.5	7.74	2
NGC 7469	23	00	44	08	36	18	Sey 1	0.017	1	520.8	9.30	1
									2	538.8	5.08	1
									3	539.4	6.96	1
MCG 2-58-22	23	02	07	-08	57	19	Sey 1	0.048	1	513.0	5.65	1
									2	519.0	9.46	1

TABLE 2

Best Fits to Single Power Law (a)

Source	Obs.	Norm.	Spectral Index (α)	Range (b)	N_H (10^{21} cm^{-2})	Range (b)	χ^2_ν (c)
III Zw 2		0.0050	0.673	0.30-1.20	1.016	0.00-3.20	0.91
Fairall.9	1	0.0098	0.998	0.90-1.50	0.000	0.00-1.40	1.19
	2	0.0089	0.675	0.55-0.95	0.000	0.00-0.80	0.99
Q0241+622		0.0074	0.789	0.40-1.15	8.75	5.40-12.6	2.26
NRAO 140		0.0053	0.907	0.75-1.15	0.00	0.00-0.50	1.51
3C 111		0.0046	-0.007	-0.40-1.05	1.655	0.00-24.0	1.23
3C 120	1	0.0171	1.091	0.92-1.42	1.857	1.15-3.25	1.26
	2	0.0083	0.444	0.32-0.75	0.000	0.00-1.50	0.97
	3	0.0039	0.203	-0.09-0.63	0.910	0.00-2.78	0.88
	4	0.0034	0.102	-0.19-0.66	0.618	0.00-3.10	0.98
	5	0.0170	1.083	0.78-1.40	2.751	1.70-3.90	1.51
MCG 8-11-11		0.0081	0.759	0.38-1.18	2.771	0.70-5.60	1.14
3C 273	1	0.0275	0.487	0.32-0.66	3.117	2.20-4.10	1.19
	2	0.0156	0.398	0.29-0.63	0.144	0.00-1.00	0.88
	3	0.0138	0.478	0.32-0.67	0.413	0.00-1.20	1.10
	4	0.0135	0.392	0.22-0.62	0.566	0.00-1.50	1.10
IC 4329A		0.0322	0.816	0.64-1.01	5.365	4.40-6.40	0.97
NGC 5548		0.0054	0.260	-0.25-1.18	1.843	0.00-7.60	0.91
3C 382		0.0032	0.108	-0.22-0.87	0.626	0.00-3.90	0.83
ESO 141-G55		0.0143	1.377	0.93-1.89	1.389	0.00-3.20	0.90
Mkn 509	1	0.0109	0.902	0.60-1.23	1.763	0.60-3.30	1.21
	2	0.0116	1.153	0.56-1.88	3.927	1.30-7.70	1.13
	3	0.0072	0.750	0.35-1.22	1.731	0.10-4.00	1.11
NGC 7469	1	0.0109	0.756	0.54-1.00	0.596	0.00-1.56	0.94
	2	0.0105	0.977	0.72-1.34	0.566	0.00-1.78	1.34
	3	0.0145	0.927	0.69-1.18	0.625	0.00-1.52	1.05
MCG 2-58-22	1	0.0074	0.575	0.30-0.98	0.782	0.00-2.41	0.98
	2	0.0065	0.495	0.40-0.78	0.008	0.00-0.98	0.73

(a) Power law spectrum is of the form dF/dE = (Norm.) x $E^{-\alpha}$ x exp $-(\sigma(E)N_H)$

keV cm^{-2} s^{-1} keV^{-1} .

(b) Range is bounded by $\chi^2_{min} + 6$.

(c) $\nu = 58$.

TABLE 3

Comparison of Spectral Indices

Source	Obs.	SSS α	SSS Range (a)	MPC (c) α	MPC (c) Range (b)	HEAO1 A-2 α	HEAO1 A-2 Range (b)	Ref.
III Zw 2		0.673	0.30-1.20	0.43	0.31-0.56			
Fairall 9	1	0.998	0.90-2.50	1.66	1.35-2.11			
	2	0.675	0.55-0.95	0.97	0.83-1.23			
Q0241+622		0.789	0.40-1.15	0.26	-0.05-0.55	0.93	0.90-0.98	d
NRAO 140		0.907	0.75-1.15	1.00	0.33-1.78			
3C 111		-0.007	-0.40-1.50	0.40	0.25-0.55	0.77	0.63-0.91	e
3C 120	1	1.036	0.87-1.40	0.74	0.67-0.82			
	2	0.444	0.32-0.75	0.83	0.70-0.97			
	3	0.203	-0.09-0.63	0.75	0.43-0.99	0.78	0.72-0.84	f
	4	0.102	-0.19-0.66					
	5	1.083	0.78-1.40	0.78	0.72-0.90			
MCG 8-11-11		0.759	0.38-1.18	1.09	0.90-1.30	0.66	0.46-0.96	g
3C 273	1	0.487	0.32-0.66	0.52	0.48-0.57			
	2	0.398	0.29-0.63					
	3	0.474	0.32-0.67	0.50	0.45-0.55	0.41	0.39-0.43	h
	4	0.392	0.22-0.62					
IC 4329A		0.816	0.64-1.01	0.68	0.63-0.73	0.76	0.66-0.96	e
NGC 5548		0.260	-0.25-1.18	0.40	0.21-0.60	0.60	0.40-1.00	g
						0.70	0.62-0.78	f
3C 382		0.108	-0.22-0.87	0.48	0.30-0.76	0.95	0.75-1.15	e
ESO 141-G55		1.377	0.93-1.89	1.14	1.02-1.26	0.80	0.40-1.20	g
Mkn 509	1	0.902	0.60-1.23	0.91	0.83-0.99			
	2	1.153	0.56-1.88	0.87	0.79-0.96	0.63	0.58-0.78	g
	3	0.750	0.35-1.22			0.64	0.60-0.68	f
NGC 7469	1	0.756	0.54-1.00	1.04	0.97-1.11			
	2	0.977	0.72-1.34	0.96	0.83-1.11	0.70	0.50-1.10	e
	3	0.927	0.69-1.18					
MCG 2-58-22	1	0.575	0.30-0.98	0.68	0.58-0.80	0.65	0.59-0.75	e
	2	0.495	0.40-0.78	0.72	0.61-0.81			

(a) $\chi^2_{min} + 6$.

(b) $\chi^2_{min} + 4.6$.

(c) Halpern (1982).

(d) Worrall et al. (1980); OSO-8.

(e) Mushotzky (1982b).

(f) Rothschild et al. (1983).

(g) Mushotzky et al. (1980).

(h) Worrall et al. (1979).

TABLE 4

Partial Covering Fraction Upper Limits

Source	Obs.	Maximum N_H (10^{21} cm^{-2})	Upper Limit on Covering Fraction	Covering Fraction (a)
III Zw 2		7.0	0.68	0.22
Fairall 9	1	2.8	0.71	0.35
	2	4.2	0.63	
3C 120	1	7.4	0.69	0.09
	2	4.5	0.58	
	3+4	7.3	0.73	
	5	5.0	0.55	
MCG 8-11-11		4.5	0.60	
3C 273	1	2.1	0.25	0.08
	2	2.2	0.29	
	3	2.0	0.30	
	4	3.6	0.36	
IC 4329A		1.4	0.42	
ESO 141-G55		5.9	0.67	0.10
Mkn 509	1	3.5	0.45	0.43
	2	8.3	0.78	
	3	3.3	0.53	
NGC 7469	1	3.3	0.43	0.24
	2	3.9	0.57	
	3	3.4	0.38	
MCG 2-58-22	1	4.8	0.57	0.46
	2	3.9	0.46	

(a) Derivation of covering fraction desecribed in §V B i.

TABLE 5

Measured 3 keV Fluxes (a)

Source	Obs.	f_3 (10^{-12} erg cm^{-2} s^{-1}) SSS	MPC (b)	HEAO1 A-2	Ref.
III Zw 2		3.85	4.12	5.6, <4.6	c
Fairall 9	1	5.28	6.59	4.4	c
	2	6.86	3.03		
Q0241+622		4.99	5.27	4.2 - 7.6	d
NRAO 140		2.93	5.82	3.5	e
3C 111		7.50	7.86	7.3	f
3C 120	1	8.34	8.78	6.6	g
	2	8.15	7.76		
	3	4.99	4.37		
	4	4.85			
	5	8.36	7.51		
MCG 8-11-11		5.78	6.40	8.6, 3.4	h
3C 273	1	25.9	22.9	19.3	i
	2	16.2	14.9		
	3	13.2	14.6		
	4	14.1	17.8		
IC 4329A		21.2	37.0	9.5	f
NGC 5548		6.56	5.70	10.0	h
3C 382		4.52	4.08	6.9	f
ESO 141-G55		5.12	5.96	8.0	h
Mkn 509	1	6.53	7.89	9.6, 7.5	h
	2	5.29	6.26		
	3	5.09	5.74		
NGC 7469	1	7.65	7.88	4.2	f
	2	5.80	6.76		
	3	8.45	9.17		
MCG 2-58-22	1	6.53	6.96	7.8	f
	2	6.05	6.96		

(a) Flux in 1 keV band centered at 3 keV.

(b) Halpern (1982).

(c) Piccionotti et al. (1982).

(d) Worrall et al. (1980).

(e) Marshall et al. (1979).

(f) Mushotzky (1983).

(g) Rothschild et al. (1983).

(h) Mushotzky et al. (1981).

(i) Worrall et al. (1979).

TABLE 5

Other Properties of Observed AGN (a)

Source	log $\langle L_{2\text{-}10} \rangle$ (b)	$\langle \alpha_{2\text{-}10} \rangle$	log (νL_ν) 3 keV	1450A (c)	3.5 μm (d)	log (Hβ) (d)	log (OIII) (d)	α_{UV} (e)
NRAO 140	46.96	0.907	46.72					
3C 273	45.81	0.438	45.65	46.70	46.24	44.38	43.18	1.1±0.1
III Zw 2	44.71	0.673	44.52	44.51	45.03	43.23	42.75	
3C 111	44.37	-0.007	44.33		44.66	42.84	42.12	
Fairall 9	44.26	0.836	44.12	44.99	44.95	43.36	42.43	
MCG 2-58-22	44.25	0.535	44.19	44.60	44.82	43.28	42.78	
3C 382	44.33	0.108	44.23					
ESO 141-G55	44.24	1.377	43.87	44.71	44.60	42.50	41.80	
Q0241+622	44.22	0.789	44.00					
Mkn 509	44.13	0.935	43.89	44.52	44.69	42.98	42.46	1.0±0.1
3C 120	44.11	0.584	43.88	43.83	44.49	42.16	42.19	
IC 4329A	43.86	0.816	43.64		44.17	41.76	41.57	
MCG 8-11-11	43.62	0.759	43.42		44.08	41.64	41.88	
NGC 7469	43.56	0.887	43.35	43.47	44.76	42.10	41.92	
NGC 5548	43.39	0.260	43.31	43.99	43.88	41.97	41.88	1.1±0.1

(a) H = 50 km s^{-1} Mpc^{-1} assumed.

(b) Intrinsic luminosity in 0.75-4.5 keV band.

(c) Wu, Boggess and Gull (1983), except 3C 273 from Ulrich et al. (1980).

(d) Lawrence and Elvis (1982).

(e) Malkan and Sargent (1982).

FIGURE CAPTIONS

Figure 1 -- Examples of 0.75-4.5 keV spectra of high X-ray luminosity active galactic nuclei from the Einstein SSS. Displayed on the left are pulse height spectra with the best fit simple spectral model (power law plus absorption) superposed. Shown on the right are the input photon spectra corresponding to the best fit model, after deconvolution from the SSS response function. Examples of all three data quality levels are displayed: IC 4329A(a,b) and MCG 2-58-22 (c,d) are quality 1; III Zw 2 (e,f) is quality 2; 3C 111 (g,h) and NRAO 140 (i,j) are quality 3.

Figure 2 -- The integral χ^2_ν distribution for a single power law fit to 28 SSS observations of high X-ray luminosity AGN. The dashed curve represents the expected integral χ^2_ν distribution for 58 degrees of freedom. Application of a Kolmogornov-Smirnov test indicates that the distribution obtained from the fits is consistent with the expected distribution at the 67 percent confidence level.

Figure 3 -- A histogram of the inferred values of the spectral index α for 28 SSS observations of 15 high X-ray luminosity AGN. The various degrees of hatching represent the three data quality levels. The "typical error" represents the 90 percent confidence limits for a quality 2 spectrum.

Figure 4 -- A comparison of inferred 0.75-4.5 spectral indices from the SSS (α_{sss}) with spectral indices at higher X-ray energies (see Table 3). (a) Inferred 1.5-10 keV spectral index from Einstein MPC (α_{MPC}) versus α_{sss}, from data collected simultaneously (Halpern

1982). A point is displayed for each observation. (b) Inferred 2-40 keV spectral index from HEAO-1 A2 ($\alpha_{\text{HEAO-1 A2}}$) versus α_{sss}. One point is plotted for each object. The open circle represents an OSO-8 measurement of the spectrum of Q0241+622.

Figure 5 -- Galactic column density plotted against column density inferred from SSS spectral measurements for 15 high X-ray luminosity AGN.

Figure 6 -- Residual column density (inferred minus galactic) for 15 high X-ray luminosity AGN. Dashed vertical line at 2×10^{21} cm^{-2} represents minimum column density measurable by the SSS in these observations. Only one object, IC 4329A, has a non-zero residual column density.

Figure 7 -- Average X-ray luminosity in 0.75-4.5 keV band $\langle L_{sss} \rangle$ versus average 0.75-4.5 spectral index $\langle \alpha_{sss} \rangle$ for 15 high X-ray luminosity AGN. Open circles represent quasars; closed circles represent Seyfert I galaxies. The solid vertical line flanked by dashed lines represents the average value and the variance of the spectral index for energies above 2 keV. No $\langle L_{sss} \rangle$ - $\langle \alpha_{sss} \rangle$ correlation exists from the entire sample or from either subset.

EXAMPLES OF SSS SPECTRA OF HIGH LUMINOSITY AGN

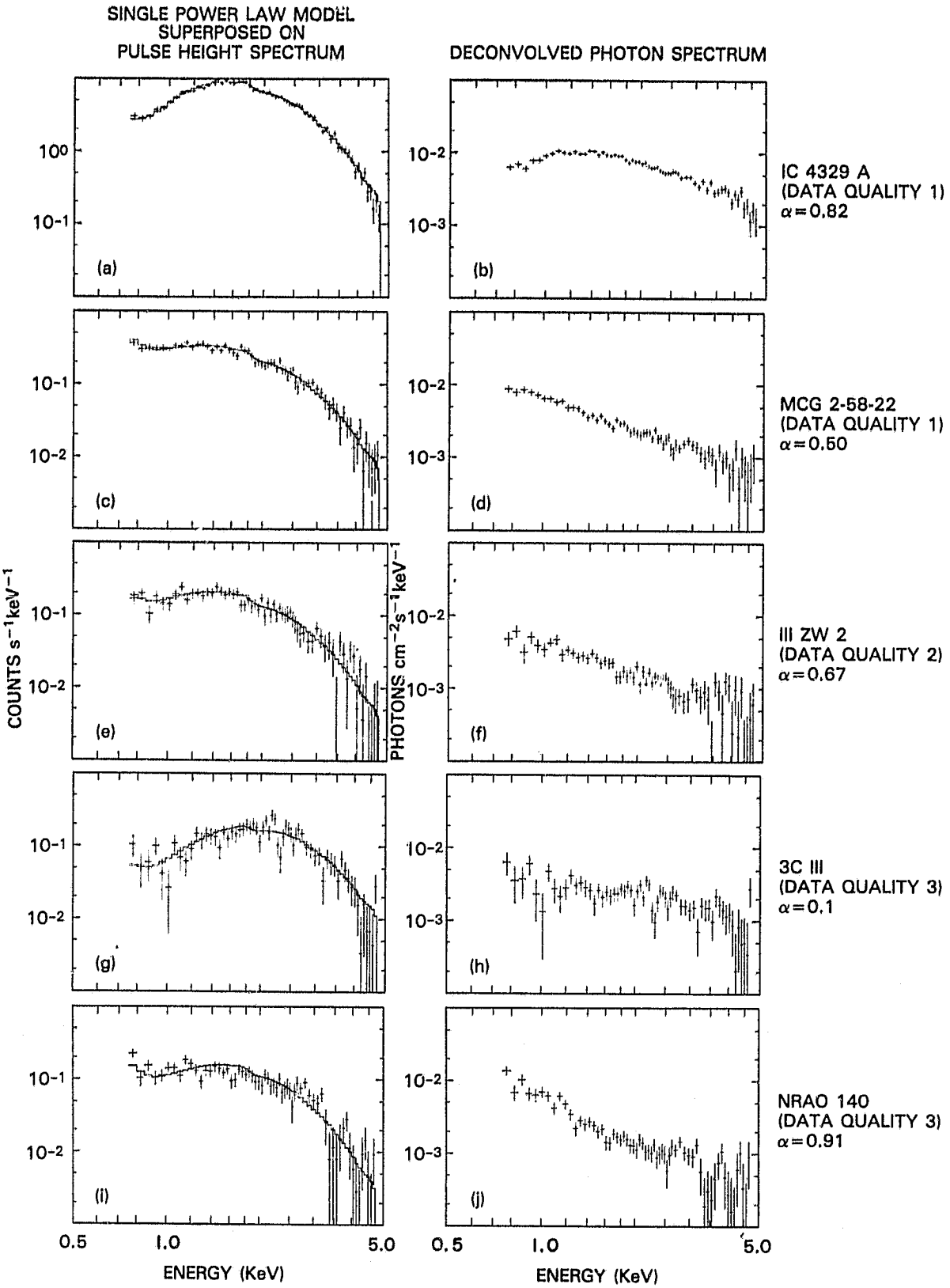

FIGURE 1

INTEGRAL χ^2_ν DISTRIBUTION FOR SINGLE POWER LAW FIT TO SSS OBSERVATIONS OF HIGH X-RAY LUMINOSITY AGN

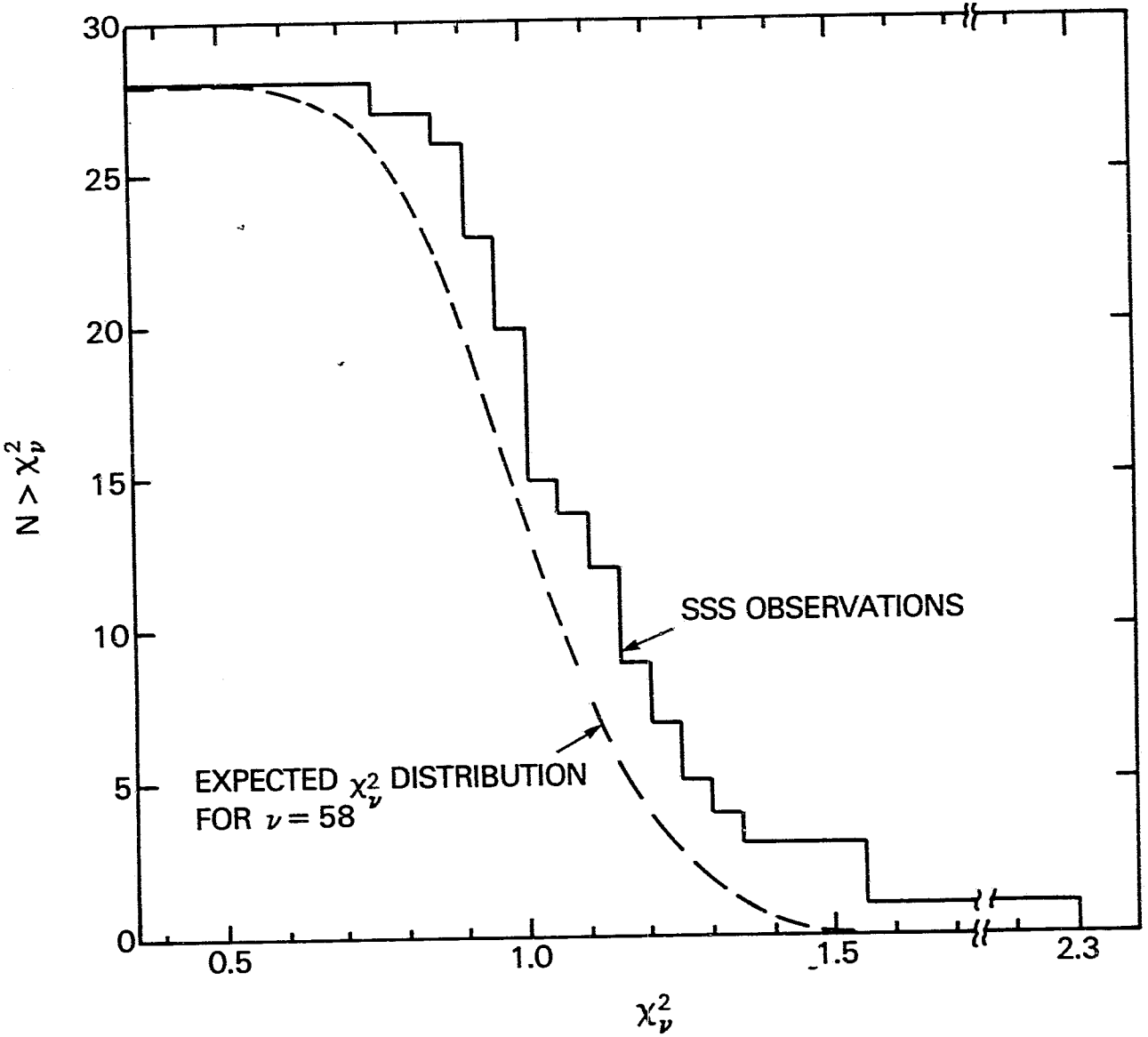

FIGURE 2

DISTRIBUTION OF SSS BAND SPECTRAL INDICES OF HIGH X-RAY LUMINOSITY AGN

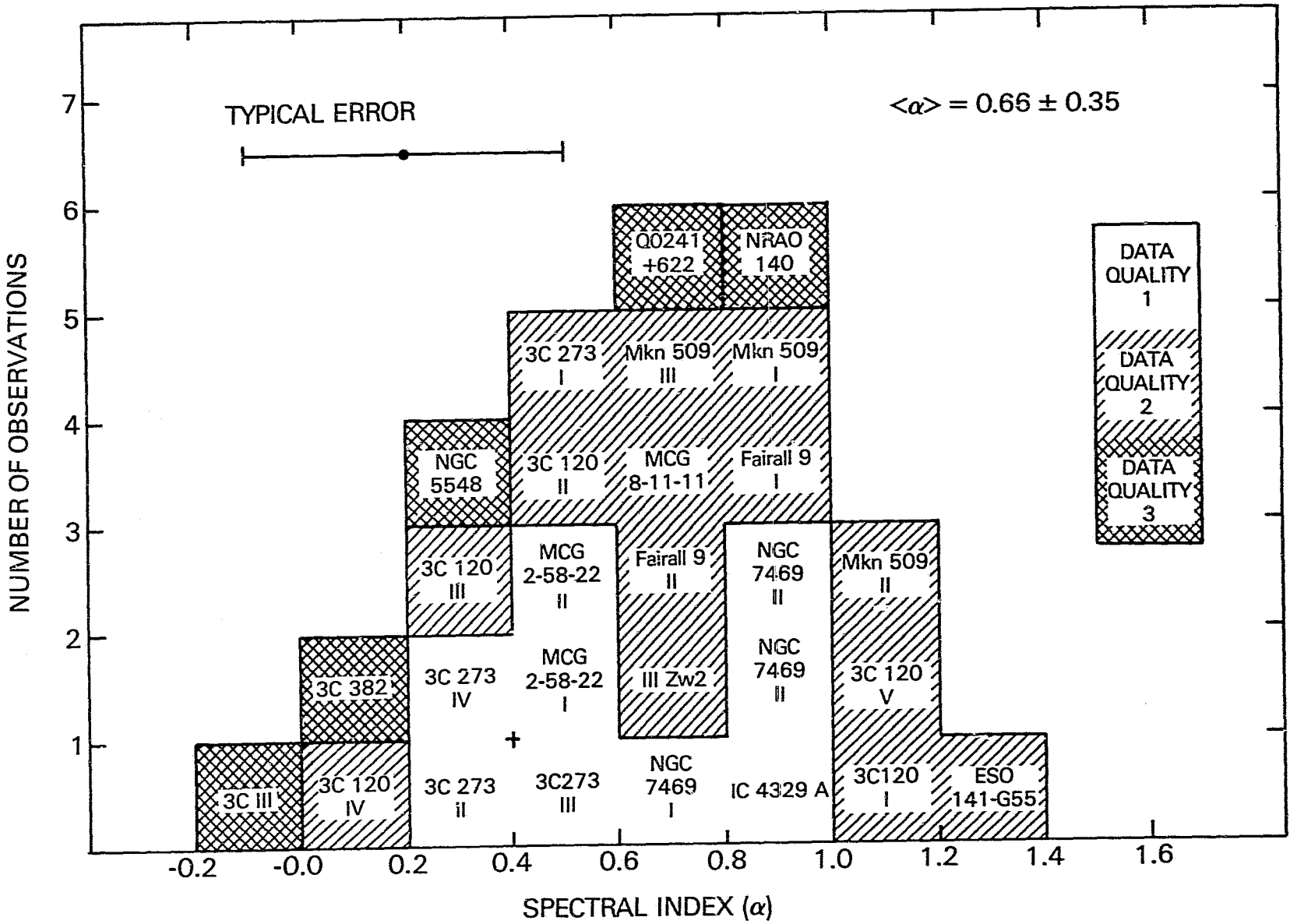

ORIGINAL PAGE IS OF POOR QUALITY

FIGURE 3

ORIGINAL PAGE IS
OF POOR QUALITY

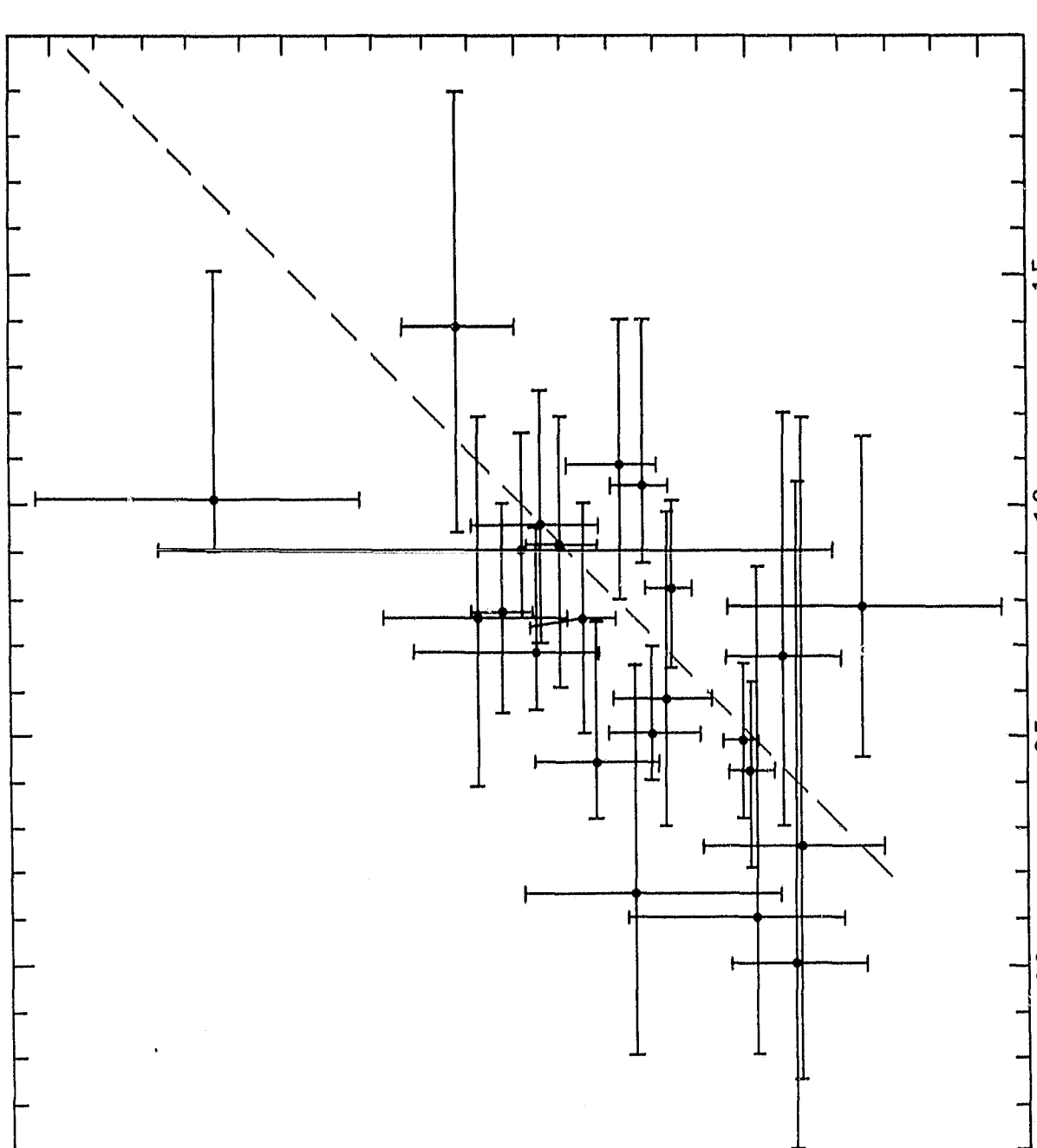

FIGURE 4a

ORIGINAL PAGE IS
OF POOR QUALITY

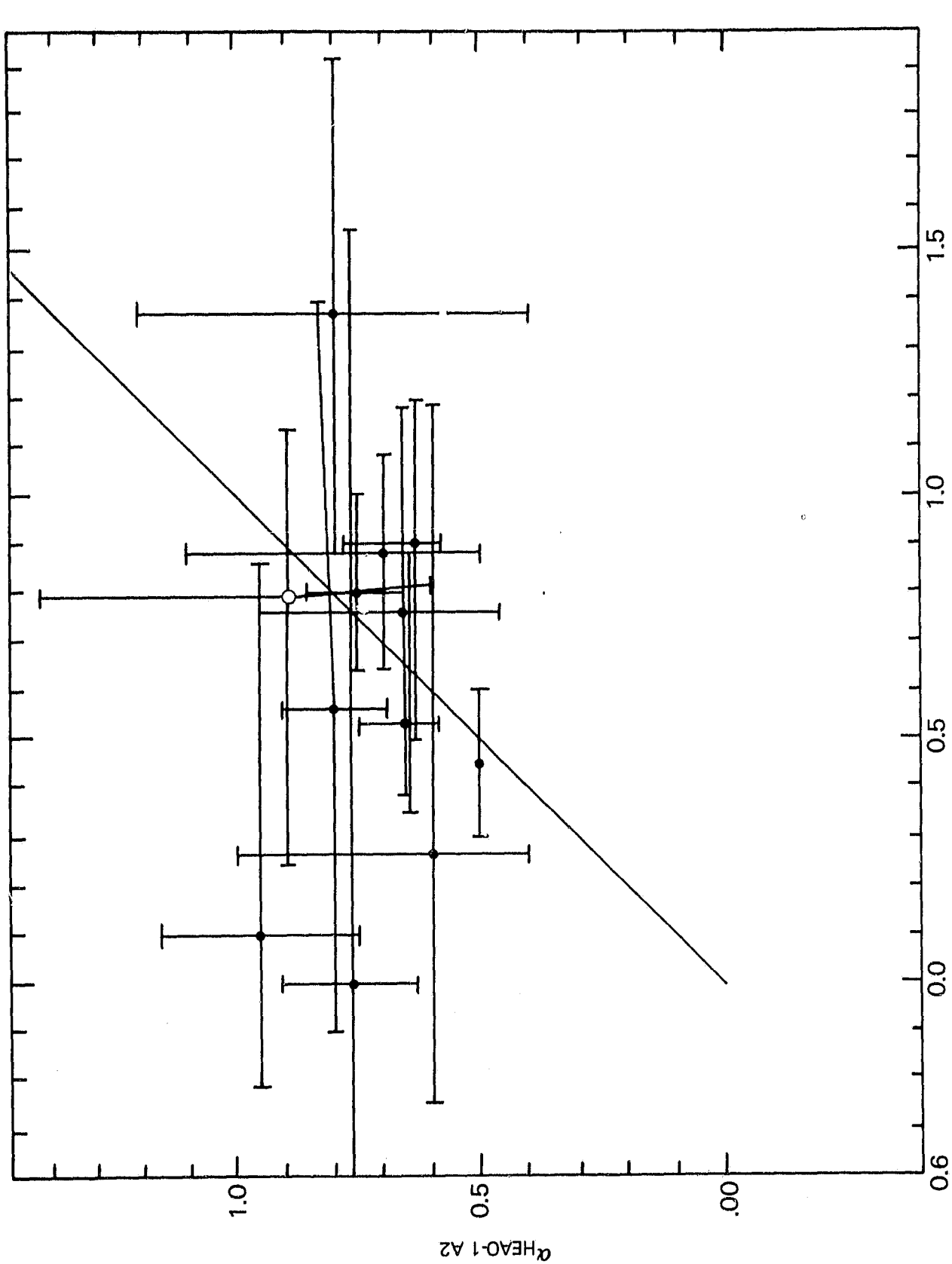

FIGURE 4b

GALACTIC COLUMN DENSITY VS. X-RAY COLUMN DENSITY FOR HIGH X-RAY LUMINOSITY AGN

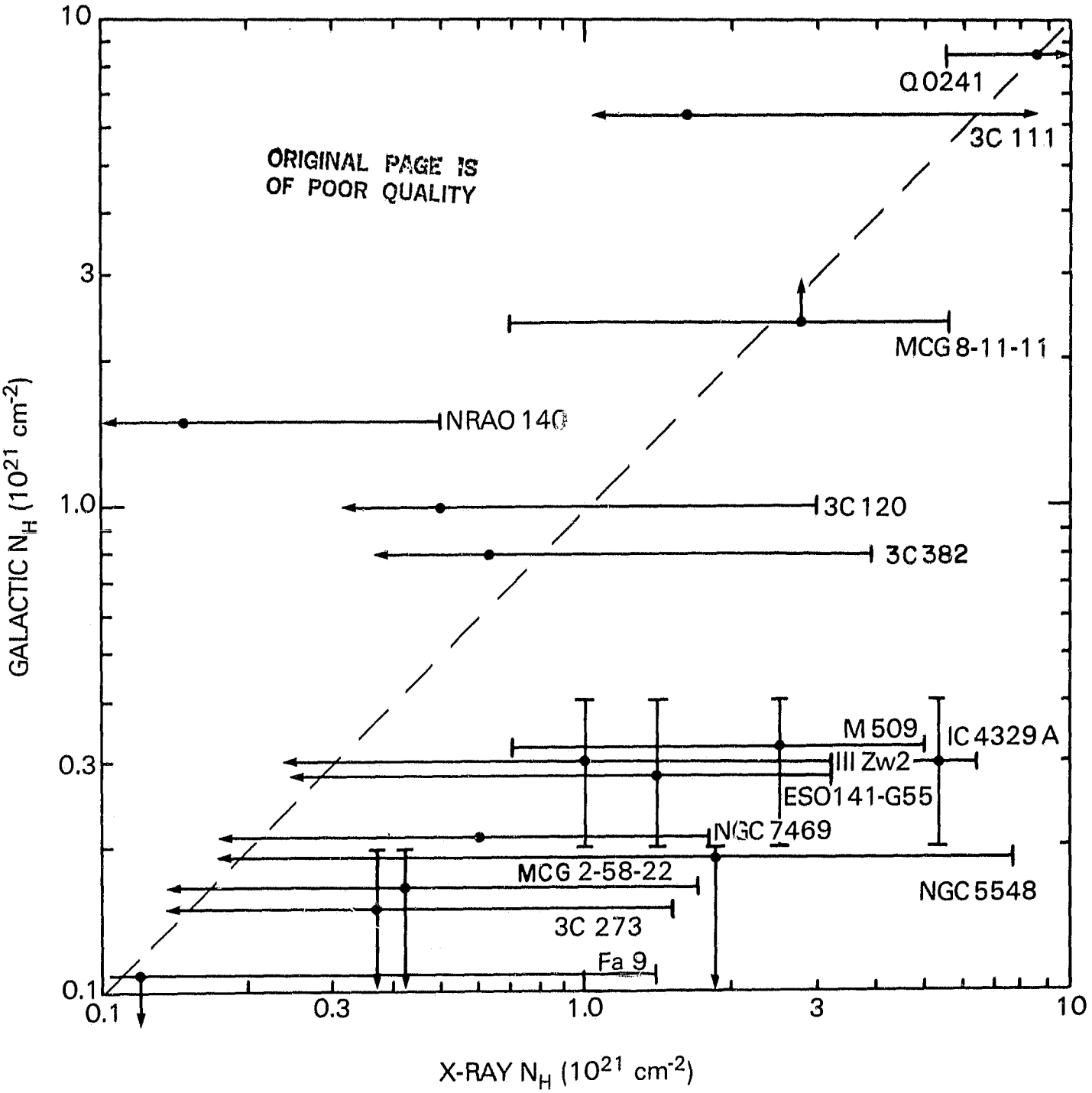

FIGURE 5

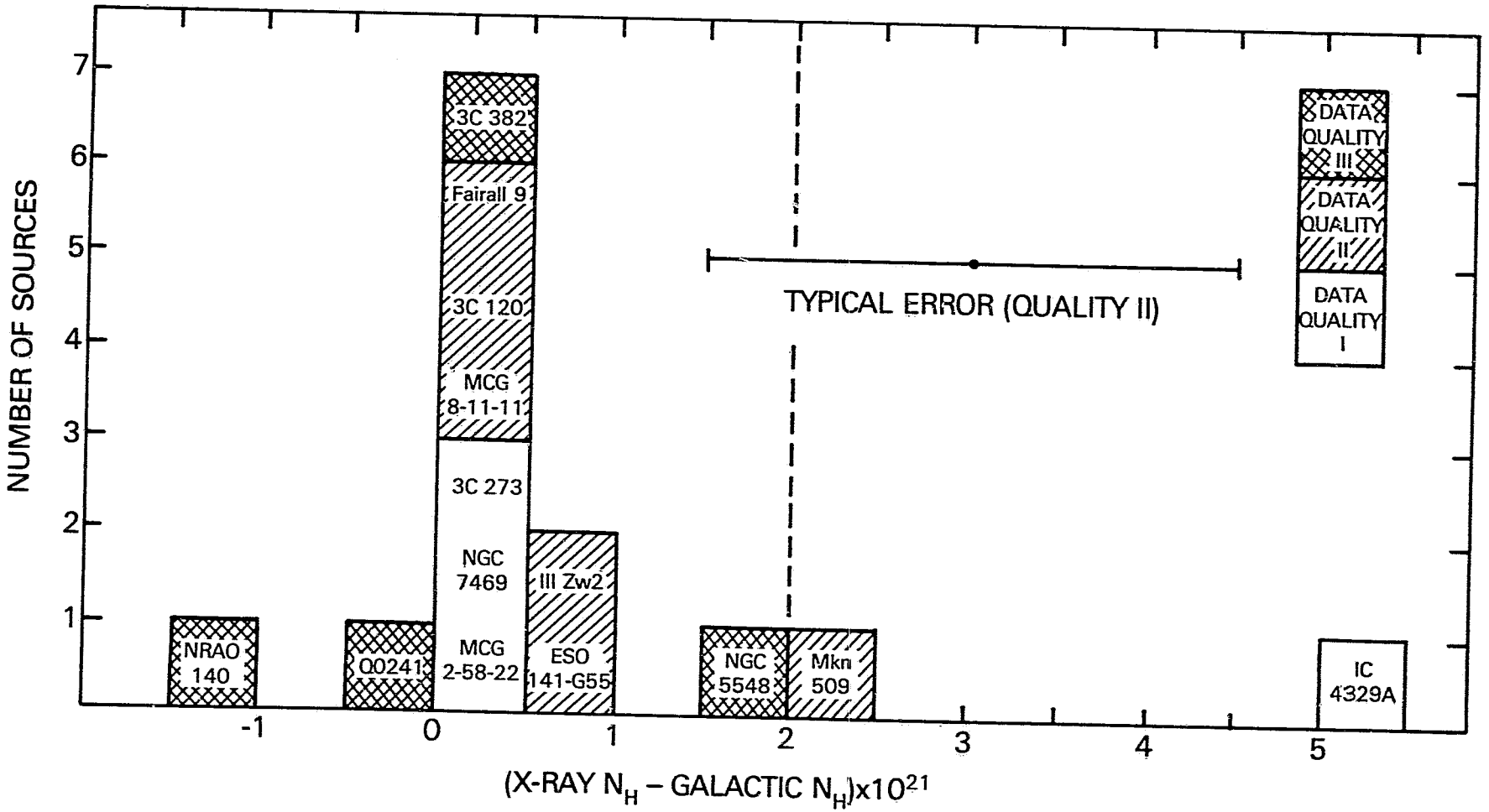

FIGURE 6

AVERAGE SOFT X-RAY LUMINOSITY VS. SPECTRAL INDEX

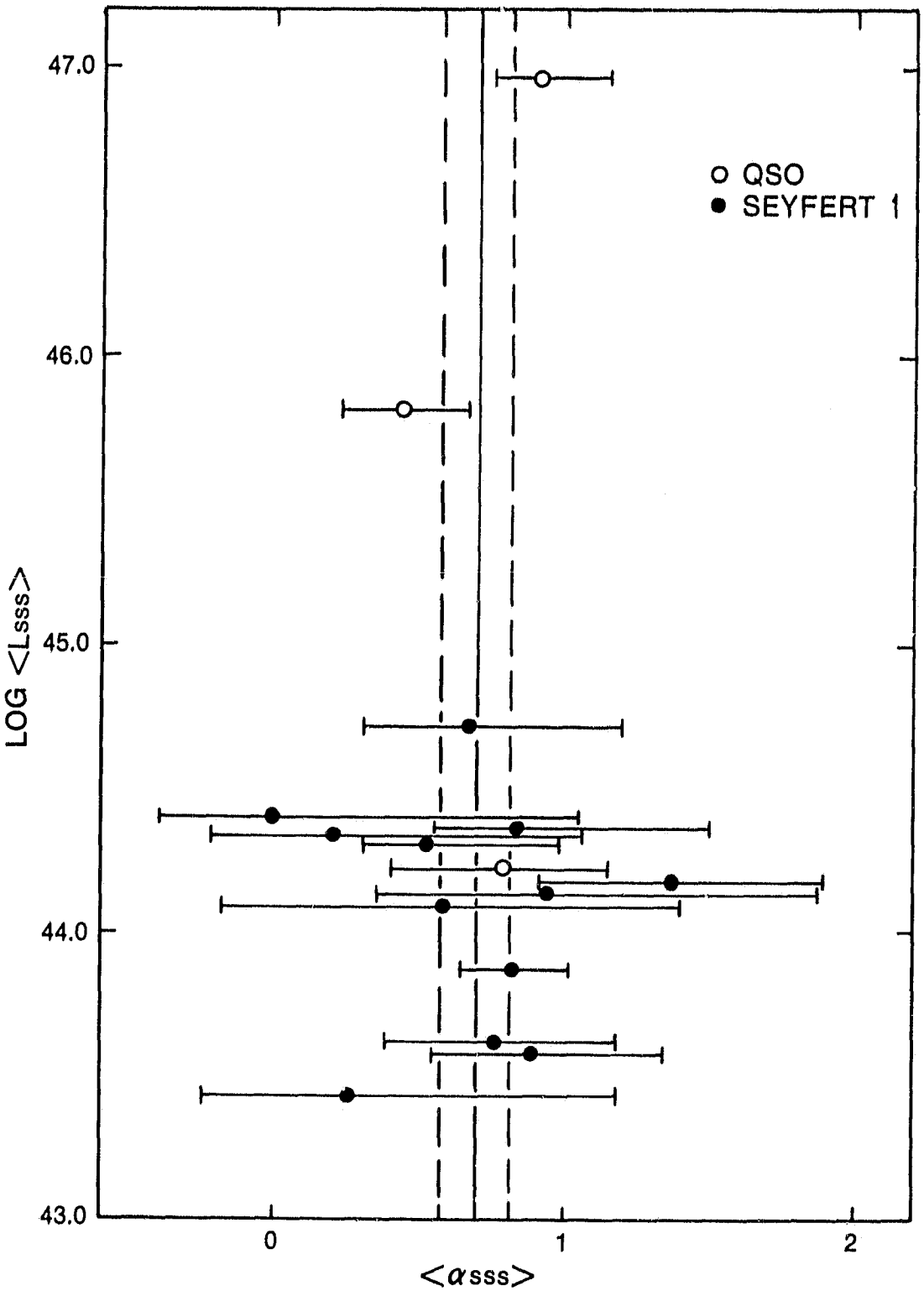

FIGURE 7

AUTHORS' ADDRESSES:

S.S. HOLT, R.F. MUSHOTZKY, and R. PETRE, Code 661, NASA/Goddard Space Flight Center, Greenbelt, MD 20771.

J.K. KROLIK, Center for Astrophysics, 60 Garden Street, Cambridge, MA 02138.